Traditional and Neural Probabilistic Multispectral Image Processing for the Dust Aerosol Detection Problem

P. Rivas-Perea, J. G. Rosiles
Department of Electrical and Computer Engineering
The University of Texas El Paso
El Paso, TX, USA
privas@miner.utep.edu, grosiles@utep.edu

M. I. Chacon M.
Graduate Studies Department
Chihuahua Institute of Technology
Chihuahua, Chih., Mexico
mchacon@ieee.org

***Abstract*—This paper address the dust aerosol detection problem based on a probabilistic multispectral image analysis. Two classifiers are designed. First the Maximum Likelihood classifier is adapted to mode different types of atmospheric components. The second is a Probabilistic Neural Network (PNN) model. The data sets are MODIS multispectral bands from NASA Terra satellite. Findings indicate that the PNN presents a better classification performance than the ML classifier using manual segmentations as ground truth. The proposed algorithm is capable of real-time processing at 1 km resolutions which is an improvement compared to the 10 km resolution currently provided by other approaches.**

***Keywords*-Maximum likelihood classification; Neural networks; Image processing; Remote sensing.**

I. Introduction

Advances in remote sensing like multispectral instruments allow imaging of atmospheric and earth materials based on their spectral signature over the optical range. In particular, dust air-borne particles (aerosols) propagated through the atmosphere in the form of dust storms can be detected through current remote sensing instruments. Dust aerosols are a major cause of health, environmental, and economical hazards, and can adversely impact urban areas [1]. From a scientific perspective, understanding dust storm genesis, formation, propagation and composition is important to reduce their impact or predict their effect (*e.g.*, increase of asthma cases).

Several methods for dust aerosol detection exist [2]. Some of the most relevant systems are based in the Moderate Resolution Spectroradiometer (MODIS) Aerosol Optical Thickness (AOT) product [3] which is provided by the NASA Terra satellite. However, AOT products require a considerable amount of processing that introduces a significant delay (*i.e.*, two days after satellite pass) before it can provide useful information on aerosol events. Other approaches are based on the so-called "band-math" [1] where simple operations between bands are used to provide a visual (and subjective) display of the presence of dust storms.

Given the large amounts of data produced by the MODIS instrument, it is also desirable to have automated systems that assists scientist on finding or classifying different earth phenomena. For example, Aksoy, *et al.* [4], developed a visual grammar scheme that integrates low-level features to provide a high level spatial scene description on land cover and land usage. As far as the authors know, similar automated schemes for dust detection based on statistical pattern recognition techniques have not been reported.

In this paper we present two methods for the detection of dust storms from multispectral imagery using statistical classifiers. Based on reported data, we present a feature set that allows high performance, accuracy, and real-time detection of dust aerosol. The proposed feature set is extracted from MODIS spectral bands and tested with the maximum likelihood classifier and the probabilistic neural network (PNN). We will show that the PNN approach provides a better detection and representation of dust storm events.

This paper is organized as follows. Section 2 of the paper introduces the dust aerosol multispectral analysis. The ML and PNN models are explained in Section 3 and 4. Section 5 presents experimental results, followed by a brief discussion on the proposed schemes. Finally, conclusions are drawn in Section 6.

II. Selection and Analysis of Spectral Bands

The MODIS instrument is part of NASA Terra satellite. MODIS data is currently used in the analysis of different phenomena like sea temperature and surface reflectivity. MODIS provides information in 36 spectral bands between wavelengths 405nm and 14.385μm. These bands are available in MODIS Level 1B file organization. In the case of dust aerosol, visual assessment can be achieved using MODIS bands $B1$, $B3$, and $B4$ which correspond to the range of human visual perception [5]. An RGB composite true color image can be produced by the mapping $R = B1$, $G = B4$, and $B = B3$. Hao *et al.* [6] demonstrated that bands $B20$,$B29$,$B31$ and $B32$ can also be utilized for dust aerosol visualization. Ackerman *et al.* [7] demonstrated that band subtraction $B32 - B31$ improves dust storm visualization contrast. Based on these findings, we will form feature

vectors using pixels values from the recovered bands $B20$, $B29$, $B31$, and $B32$.

A "recovered" radiance is a 16 bit MODIS band recovered to its original units ($W/m^2/\mu m/sr$). The recovery process is given by

$$L = \kappa(\iota - \eta), \tag{1}$$

where L denotes the recovered radiance, κ is the radiance scale, η denotes the radiance offset, and ι is the scaled intensity (raw data). For each pixel location (n, m), our feature vector $F \in \Re^4$ consist of the following recovered radiances

$$F_{nm} = \left[L_{nm}^{B20}, L_{nm}^{B29}, L_{nm}^{B31}, L_{nm}^{B32}\right]^T. \tag{2}$$

corresponding to the dust sensitive wavelengths.

In our experiments we selected 31 different events corresponding to the south-western US, and north-western Mexico area. The 31 events are known dust storm cases reported in [8]. From these events, 23 were selected to train and test the classifiers. Each event contains multispectral images of size 2030×1053 pixels. We manually segmented the images into four classes $C = \{\textit{dust storm}, \textit{blowing dust}, \textit{smoke}, \textit{background}\}$. The selection of modeling (training) and testing feature vectors was performed randomly over the class sets. The complete data set provides approximately 75 million feature vectors from which 97.5% correspond to the background class.

III. Dust Storm Detection using the Maximum Likelihood Classifier

The Maximum Likelihood Classifier (ML) has been extensively studied in remotely sensed data classification and analysis [4], [9]. Here we present a straightforward adaptation of the ML classifier to dust storm detection using the feature set described in the previous section. Let $f_{X|k}(x) = (X = x|C = k)$ be the conditional probability density function of feature vector X having a value x, given the probability that the k-th class occurs. This might be referred as the "data likelihood" function. Assuming normally distributed features (*i.e.*, pixel values), we can define a discriminant function

$$\psi_k(x) = -\det\left(\mathbf{\Sigma}_k\right) - \left(x - \mu_k\right)^T \mathbf{\Sigma}_k^{-1} \left(x - \mu_k\right) \tag{3}$$

for each class k, where $\mathbf{\Sigma}_k$ the covariance matrix, μ_k denotes the mean feature vector, and $\det(\cdot)$ is the determinant function. Then, the decision rule can be simply stated as

$$x \in C = j \quad \text{if} \quad \psi_j(x) > \psi_i(x) \quad \forall j \neq i. \tag{4}$$

The parameters $\mathbf{\Sigma}_k$ and μ_k were obtained from the training data described in the previous section using the maximum likelihood estimators (*e.g.*, sample mean and sample covariance matrix).

IV. Neuro-Probabilistic Modeling: The Probabilistic Neural Network

Specht's Probabilistic Neural Network (PNN) is a semi-supervised neural network [10]. It is widely used in pattern recognition applications [11]. The PNN is inspired in Bayesian classification and does not require training. It estimate the PDF of each feature assuming they are normally distributed. The PNN has a four-layered architecture. The first layer is an input layer receiving the feature vectors F_{nm}. The second layer consists of a set of neurons which are fully connected to the input nodes. The output of this layer is given by

$$\varphi_{jk}\left(F\right) = \frac{1}{\left(2\pi\right)^{\frac{d}{2}} \sigma^d} e^{-\frac{1}{2\sigma^2}\left(F - \nu_{jk}^F\right)^T \left(F - \nu_{jk}^F\right)}. \tag{5}$$

where j is an index labeling each design vector and k is its the corresponding class. The pattern units ν_{jk}^F correspond to the mean feature vector for each class. The parameter σ is estimated with the method developed by Srinivasan *et al.* [12].

The third layer contains summation units to complete the probability estimation. There are as many summation units as classes. The $j-th$ summation unit denoted as $\Omega_j(\cdot)$, receives input only from those pattern units belonging to the $j-th$ class. This layer computes the likelihood of F being classified as C, averaging and summarizing the output of neurons belonging to the same class. This can be expressed as

$$\Omega_j\left(\varphi_{jk}\left(F\right)\right) = \frac{1}{\left(2\pi\right)^{\frac{d}{2}} \sigma^d} \frac{1}{N_j} \times \ldots \sum_{i=1}^{N_j} e^{-\frac{1}{2\sigma^2}\left(\varphi_{ik}(F) - \varpi_i\right)^T \left(\varphi_{ik}(F) - \varpi_i\right)}. \tag{6}$$

The last layer classifies feature input vector F_{nm} according to the Bayesian decision rule given by

$$F \in C_j \text{ if, } \ldots \quad C_j\left(\Omega_j\left(\varphi_{jk}\left(F\right)\right)\right) = \arg\max_{1 \leq i \leq j} \Omega_i\left(\varphi_{ik}\left(F\right)\right). \tag{7}$$

A. The PNN Large Sample Size Problem

To avoid the overwhelming processing of millions training samples, we limited the training samples number. We based our reduction method on Kanellopoulos criteria [13] which establishes that the number of training samples must be at least three times the number of feature bands. Therefore, in our PNN design we used six times the feature vector size (*e.g.*, four) requiring 24 training samples per class. In order to select the testing vectors (24 per class), principal component analysis (PCA) was applied to a training set consisting of millions of feature vectors. Then the test feature vectors associated to the 24 largest eigenvalues were selected as the PNN training set.

V. Results and Discussion

The performance metrics used to compare the two classification methods are based on the number of "True Positives" (TP). "False Positives" (FP), "True Negatives" (TN), and "False Negatives" (FN). The three performance metrics are defined as

$$\text{Precision} = \frac{\sum TP}{\sum TP + FP}, \quad (8)$$

$$\text{Accuracy} = \frac{\sum TP + TN}{\sum TP + FN + FP + TN}, \quad (9)$$

as well as the area under the curve (AUC) of the receiver operating characteristics (ROC). AUC is widely used metric because its superiority in reflecting the true performance of a classification system [14].

The numerical results were concentrated and averaged to produce Table I, showing that the neuro-probabilistic approach is better than the ML. A higher precision and accuracy reflects that a system produce more true positives results and also reduces the number of false negatives. A higher AUC reflects how a classifier is able to correctly classify feature vectors and at the same time minimize the missclassification errors.

The processing time is an important measure when modeling real-time processing systems. In the case of the MODIS instrument, a complete scan (10×1053 pixels) is produced every 6.25 seconds. Thus, a real-time system must perform a classification in less than or equal to this time. Table I shows the processing time per scan in seconds. Therefore, since ML approach takes less than one second to classify the complete scan, and the PNN approach takes about 2.5 seconds to produce the classification result, both can be considered suitable for real time detections at 1km resolution. In contrast, the MODIS AOT product takes two days to be produced and released at a 10km resolution.

To perform a visual assessment of the results, consider the dust storm event on April 6th, 2001, shown in Figure 1. Visual results of the classification for ML and PNN are illustrated in Figure 2 and Figure 3 respectively. The segmentation shown in Figures 2 and 3 maps *dust storm* to red, *blowing dust* to green, *smoke* to blue, and *background* to black. Visually, both the ML and PNN approaches correctly classify the dust storm pixels.

Dust storm aerosols spread across large geographic areas is commonly referred to as the "dust transport". The dust transport is studied to see the origins and extensions of a dust storm. Problems arise when trying to observe the dust transport since the dust aerosol concentration is reduced as the storm advances. However, the dust storm transport can be studied by analyzing the pixels classified as dust storm but with lower probability. This can be easily achieved by a mapping of pixel probabilities to the image of either the ML or PNN classifiers, as shown in Figure 4. This mapping can be produced by observing the probabilities associated to the final classification of a feature vector. These probabilities are obtained with (3) and (6) for ML and PNN respectively.

Table I
Classifiers Performance.

	Precision	Accuracy	AUC	P. Time
ML	0.5255	0.6779	0.4884	0.1484
PNN	0.7664	0.8412	0.6293	2.5198

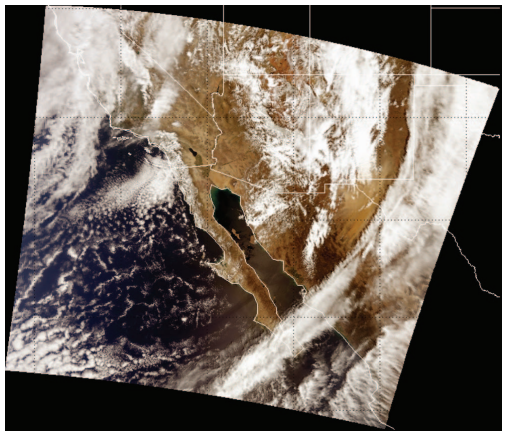

Figure 1. Dust storm event on April 6th 2001. True color image.

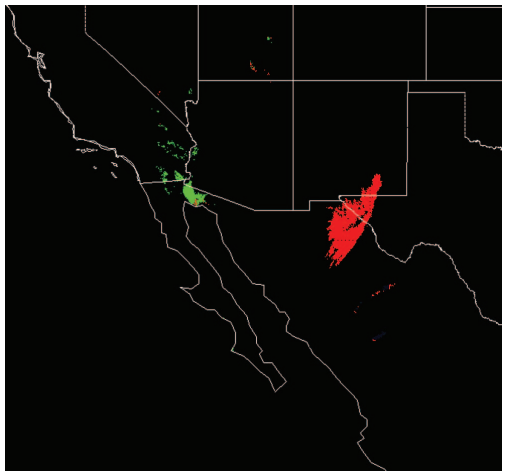

Figure 2. Dust storm event on April 6th 2001. Segmentation with ML.

VI. Conclusion

The dust aerosol detection problem has been addressed in this paper. We have modeled probabilistic approaches for dust storm detection and classification. These models are specialized on measuring the dust aerosol probability given MODIS Level 1B data. Novel Machine Learning techniques were utilized to model a dust aerosol detection neural architecture. To the best of the authors knowledge, the presented work is first in its kind. We compared the Maximum Likelihood classification (ML) model, and the

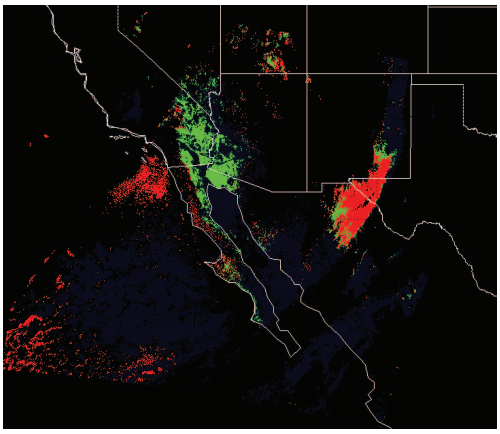

Figure 3. Dust storm event on April 6th 2001. Segmentation with PNN.

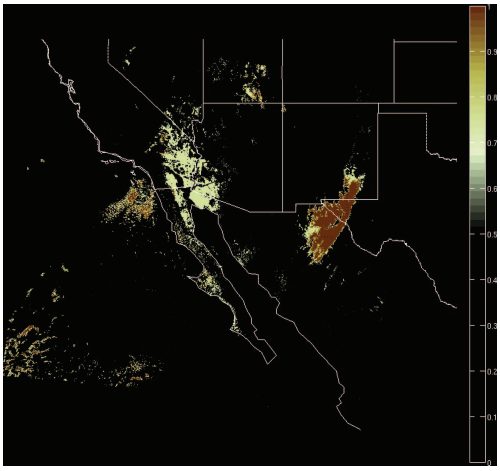

Figure 4. Dust storm event on April 6th 2001. Dust probability with PNN.

Probabilistic Neural Network (PNN). The PNN showed a strong inference ability classifying dust, and discriminating other classes, such as clouds, smoke, and background. Moreover, the proposed probabilistic models are suitable for near real-time applications, such as direct broadcast, rapid response analysis, emergency alerts, etc. The reported work has relevancy in dust aerosol analysis, since the algorithms can show the dust presence to a resolution of 1km. This represents an improvement over Aerosol Optical Thickness index (AOT) methods, which lack of resolution, and have a two day generation delay.

ACKNOWLEDGMENT

The author P.R.P performed the work while at NASA Goddard Space Flight Center under the Graduate Student Summer Program (GSSP). This work was partially supported by the National Council for Science and Technology (CONACyT), Mexico, under grant 193324/303732, as well as by the University of Texas El Paso Graduate School Cotton Memorial Funding. The author M.I.C.M. wants to thank DGEST for the support in the dust storm project.

REFERENCES

[1] Rivera Rivera, N.I., Gebhart, K.A., Gill, T.E., Hand, J.L., Novlan, D.J., and Fitzgerald, R.M., 2009. "Analysis of air transport patterns bringing dust storms to El Paso, Texas." Symposium on Urban High Impact Weather, AMS Annual Meeting, January 2009, Phoenix., JP2.6.

[2] Khazenie, N.; Lee, T.F., "Identification Of Aerosol Features Such As Smoke And Dust, In NOAA-AVHRR Data Using Spatial Textures," Geosc. and Rem. Sens. Symp., May 1992.

[3] Levy, R.C., Remer, L.A., Kaufman, Y.J., Tanr, D., Mattoo, S., Vermote, E. and O. Dubovik, "Revised Algorithm Theoretical Basis Document: MODIS Aerosol Products MOD/MYD04." 2006.

[4] Aksoy, S.; Koperski, K.; Tusk, C.; Marchisio, G.; Tilton, J.C., "Learning bayesian classifiers for scene classification with a visual grammar," Geosc. and Rem. Sens., IEEE Trans. on, vol.43, no.3, pp. 581-589, 2005.

[5] Gumley L., Descloitres J., and Schmaltz J. "Creating Reprojected True Color MODIS Images: A Tutorial." Technical Report. Version: 1.0.2, 14 January 2010.

[6] Xianjun Hao, John J. Qu, 2007, "Saharan dust storm detection using MODIS thermal infrared bands." Journal of Applied Remote Sensing, Vol. 1, pp. 013510.

[7] Ackerman, S.A., Strabala, K.I., Menzel, W.P., Frey, R., Moeller, C., Gumley, L., Baum, B.A., Seeman, S.W., and Zhang, H.. "Discriminating clear-sky from cloud with MODIS algorithm theoretical basis document (MOD35)." ATBD-MOD-06, version 4.0, NASA Goddard Space Flight Center.

[8] D. J. Novlan, M. Hardiman, and T. E. Gill, "A synoptic climatology of blowing dust events in El Paso, Texas", 16th Conference on Applied Climatology, AMS, J3.12, pp. 13

[9] John A. Richards and Xiuping Jia, "Remote Sensing Digital Image Analysis," Springer, 2006.

[10] D. F. Specht, "Probabilistic neural networks for classification, mapping, or associative memory," IEEE international conference on neural networks, vol. 1, num. 7, pp. 525-532, 1988.

[11] R. O. Duda, P. E. Hart, and D. G. Stork, "Pattern Classification," New York, John Wiley and Sons, 2001, pp. 1 - 654, ISBN 0-471-05669-3.

[12] Ramakrishnan, S. and Selvan, S. "Image texture classification using wavelet based curve fitting and probabilistic neural network." Int. J. Imaging Syst. Technol. pp. 266-275. 2007.

[13] Kanellopoulos, G. G. Wilkinson, J. Austin, "Neurocomputation in Remote Sensing Data Analysis," Springer-Verlag, 1997.

[14] J. A. Hanley, and B. J. McNeil, "The meaning and use of the area under a receiver operating characteristic (ROC) curve." Radiology, vol. 143, no. 1, pp=29, 1982.